XIV International Conference on Topics in Astroparticle and Underground Physics (TAUP 2015) IOP Publishing
Journal of Physics: Conference Series **718** (2016) 042057 doi:10.1088/1742-6596/718/4/042057

Measurement of radioactive contamination in the CCD's of the DAMIC experiment

A Aguilar-Arevalo[a], D Amidei[b], X Bertou[c], D Bole[b], M Butner[d,j], G Cancelo[d], A Castañeda Vásquez[a], A E Chavarria[e], J R T de Mello Neto[f], S Dixon[e], J C D'Olivo[a], J Estrada[d], G Fernandez Moroni[d], K P Hernández Torres[a], F Izraelevitch[d], A Kavner[b], B Kilminster[g], I Lawson[h], J Liao[g], M López[i], J Molina[i], G Moreno-Granados[a], J Pena[e], P Privitera[e], Y Sarkis[a], V Scarpine[d], T Schwarz[b], M Sofo Haro[c], J Tiffenberg[d], D Torres Machado[f*], F Trillaud[a], X You[f] and J Zhou[e]

[a] Universidad Nacional Autónoma de México, México D.F., México
[b] University of Michigan, Department of Physics, Ann Arbor, MI, U.S.A.
[c] Centro Atómico Bariloche - Instituto Balseiro, CNEA/CONICET, Argentina
[d] Fermi National Accelerator Laboratory, Batavia, IL, U.S.A.
[e] Kavli Institute for Cosmological Physics and The Eurico Fermi Institute, The University of Chicago, Chicago, IL, U.S.A.
[f] Universidade Federal do Rio de Janeiro, Instituto de Física, Rio de Janeiro, RJ, Brazil
[g] Universität Zürich Physik Institut, Zurich, Switzerland
[h] SNOLAB, Lively, ON, Canada
[i] Facultad de Ingeniería - Universidad Nacional de Asunción, Paraguay
[j] Northern Illinois University, DeKalb, IL, U.S.A.

E-mail: `torres@if.ufrj.br`

Abstract.
DAMIC (Dark Matter in CCDs) is an experiment searching for dark matter particles employing fully-depleted charge-coupled devices. Using the bulk silicon which composes the detector as target, we expect to observe coherent WIMP-nucleus elastic scattering. Although located in the SNOLAB laboratory, 2 km below the surface, the CCDs are not completely free of radioactive contamination, in particular coming from radon daughters or from the detector itself. We present novel techniques for the measurement of the radioactive contamination in the bulk silicon and on the surface of DAMIC CCDs. Limits on the Uranium and Thorium contamination as well as on the cosmogenic isotope ^{32}Si, intrinsically present on the detector, were performed. We have obtained upper limits on the ^{238}U (^{232}Th) decay rate of 5 (15) kg^{-1}d^{-1} at 95% CL. Pairs of spatially correlated electron tracks expected from ^{32}Si-^{32}P and ^{210}Pb-^{210}Bi beta decays were also measured. We have found a decay rate of 80^{+110}_{-65} kg^{-1}d^{-1} for ^{32}Si and an upper limit of ~ 35 kg^{-1}d^{-1} for ^{210}Pb, both at 95% CL.

1. Introduction

The DAMIC experiment [1] employs fully-depleted charge-coupled devices to detect WIMPs. The very low energy threshold and background level make the CCDs, composed of ultra-pure silicon, an ideal instrument to probe ∼1-20 GeV WIMPs [2, 3]. To compensate the modest mass

of the CCDs, background levels must be kept as low as possible and stable over time in order to increase the significance of the results. Because the SNOLAB is located at ∼2 km below the surface, the flux of cosmic ray-induced muons is strongly suppressed. Likewise, the shielding around the detector reduces dramatically others sources of background such as x-rays or low energy neutrons. Nevertheless, some sources of background intrinsically related to the detector cannot be easily removed and must be quantified. In this analysis we exploit the high spatial resolution of the CCDs to derive signatures for α and β particles and to identify the radioactive decay chains.

2. The DAMIC CCDs

The DAMIC CCDs [4] feature a three-phase polysilicon gate structure with a buried p-channel. The pixel size is $15\mu\text{m} \times 15\mu\text{m}$ and the active region of the detector is high-resistivity ($10 - 20\,\text{k}\Omega\text{cm}$) n-type silicon hundreds of micrometers thick. The high-resistivity of the silicon allows for a low donor density in the substrate ($\sim 10^{11}\text{cm}^{-3}$), which leads to fully depleted operation at reasonably low values of the applied bias voltage (∼40 V for a 675μm-thick CCD). The CCDs are typically 8 or 16 Mpixels, with surface areas of tens of square centimeters.

Ionization produced in the bulk of the CCD is drifted along the direction of the electric field (z-axis). The charge carriers are collected and held near the p-n junction. Due to the mobility of the charge carriers, the ionized charge will diffuse as it is drifted, with a spatial variance that is proportional to the carrier transit time. Charge produced by interactions close to the back of the CCD will have longer transit times, leading to greater lateral diffusion. The lateral spread of the charge recorded on the CCD x-y plane may be used to reconstruct the z-coordinate of a point-like interaction. For extended tracks (electrons, muons), this effect leads to a greater width when the track is closer to the backside, which provides information on the track orientation (figure 1). Further details about the CCDs performance and the setup at SNOLAB can be found in [5] and [6].

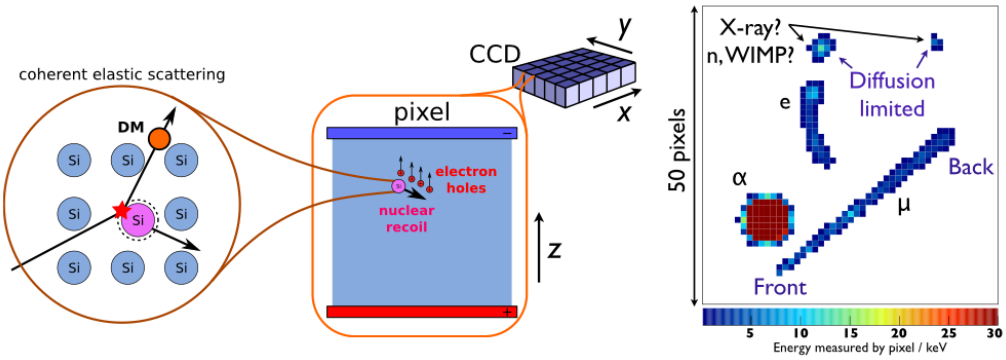

Figure 1. Left: WIMP detection principle, where the scattering of a dark matter particle with a Si nucleus leads to ionization being produced in the bulk silicon. **Right:** Segment of a DAMIC image when exposed to a ^{252}Cf source on the surface. Low energy electrons, x-rays and nuclear recoils produce diffusion limited clusters. High energy electrons (e) lead to extended tracks. α particles in the bulk or from the back of the CCD produce large round structures due to the plasma effect. Cosmic muons (μ) pierce through the CCD, leaving a straight track.

3. Limits on uranium and thorium contamination from α spectroscopy

Radioactive elements and their fission products maybe be present in the CCDs, in the electrical elements of the device, and in the air surrounding it. Thanks to the high spatial resolution of the CCDs, decay sequences of alpha particles can be quantified unambiguously. The first step in such an analysis is to determine the depth of interaction of the α's particle. We exploit the fact that α's created on the bulk or in the back of the CCDs produce highly-diffuse round clusters of hundreds of micrometers in diameter, due to the plasma effect [7]. On the other hand, α's produced in the front of the CCD deposit their energy less than 20 μm below the gates and can hardly overcome the potential barrier of the vertical channel stops between columns. This phenomenon is know as blooming and leads to mostly vertical clusters.

Criteria based on the shape of the tracks are used to distinguish α from β particles. Here we determine the smallest rectangular box that contain a cluster and compute the fraction of pixels, f_{pix} in this box. For symmetric clusters (i.e. α's) f_{pix} is large ($\sim \pi/4$ for a round cluster). For the long and irregularly shaped worms characteristic of electrons, f_{pix} is small and decreases with increasing energy. To distinguish plasma from bloomed α's, the spatial RMS $\sigma_{x,y}$ of the cluster is computed. As plasma α's have a round-shaped cluster, $\sigma_x/\sigma_y \sim 1$, while bloomed α's are generally longer along the y axis, giving $\sigma_x/\sigma_y < 1$ (see figure 2). Finally, we use the variable $N_{pix}\sigma_x/\sigma_y$ to separate plasma from bloomed α's, where N_{pix} is the number of pixels belonging to the cluster.

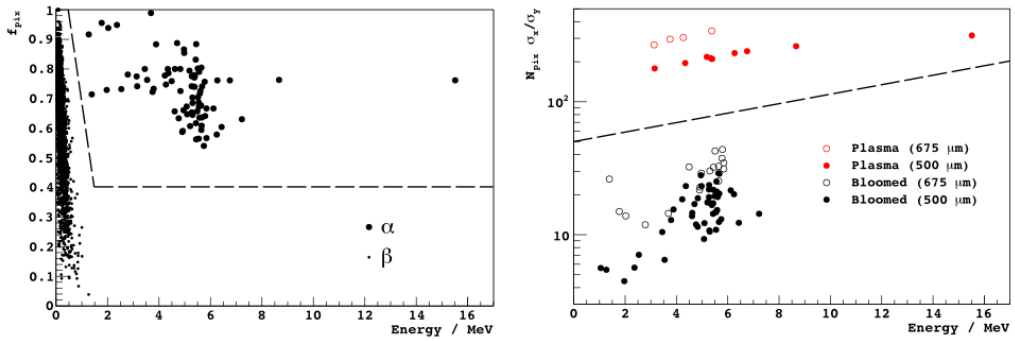

Figure 2. Left: The fraction f_{pix} as function of the cluster energy. The clusters above the dashed line are selected as α's. **Right:** The variable $N_{pix}\sigma_x/\sigma_y$ as function of the α energy. The distribution of $N_{pix}\sigma_x/\sigma_y$ for plasma and bloomed α's are clearly distinguishable for both 500 and 675 μm-thick CCDs.

Most of the bloomed α's are clustered around the characteristic energy of ^{210}Po (5.3 MeV), which may indicate a surface contamination due to ^{222}Rn. Several α's have energy < 4 MeV, lower than any α's from the ^{238}U or ^{232}Th chains. Most likely, these are α's which lose some energy before reaching the active region of the device, and originate from surface contamination of the CCD or nearby materials. Assuming that all bloomed α's with energy < 6 MeV are due to ^{210}Po decays from ^{210}Pb contamination on the front surface of the CCD, we obtain an activity of $0.078 \pm 0.010\,\mathrm{cm}^{-2}\mathrm{d}^{-1}$. Likewise, making the assumption that the plasma α's with energy < 6 MeV originate from ^{210}Po back-surface, we obtain an activity of $0.012 \pm 0.004\,\mathrm{cm}^{-2}\mathrm{d}^{-1}$.

As shown in figure 3, we have observed α sequences starting roughly in the same x-y position in different CCD images. Since the accidental probability of this occurrence is negligible, they should have a common origin. A likely explanation is that we have observed a decay sequence starting with a ^{228}Th nucleus. The energies of the α's and the time separation between decays are consistent with those from the decays of ^{228}Th, ^{216}Po and ^{212}Po. The two other α's of

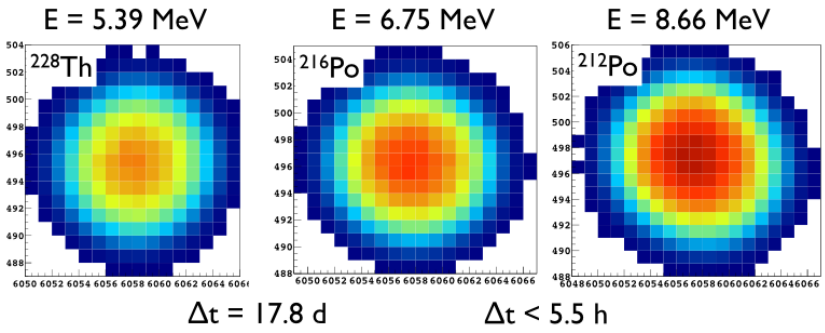

Figure 3. Three α particles detected in different CCD images at the same x-y position. Their energies and the time separation between images are consistent with a sequence from a ^{232}Th decay chain.

the sequence (^{224}Ra and ^{220}Rn) must have been emitted away from the CCD and thus gone undetected.

4. Limits on ^{32}Si and ^{210}Pb from β decay sequences

A similar search can be performed in order to find traces of ^{32}Si and ^{210}Pb through sequences of β decays. As their spectra extend to the keV-scale energies, they can represent a significant background in the region of interest for the WIMP search. For dark matter silicon-based detectors such as DAMIC or CDMS [8], the isotope ^{32}Si is particularly dangerous due to its content in the raw silica. It leads to the following decay sequence:

$$^{32}\mathrm{Si} \longrightarrow {}^{32}\mathrm{P} + \beta^{-}(\tau_{1/2} = 150\,\mathrm{y}, \mathrm{Q} = 227\,\mathrm{keV}), \quad (1)$$

$$^{32}\mathrm{P} \longrightarrow {}^{32}\mathrm{S} + \beta^{-}(\tau_{1/2} = 14\,\mathrm{d}, \mathrm{Q} = 1.71\,\mathrm{MeV}). \quad (2)$$

In this case, the intermediate nuclei, ^{32}P, is expected to remain in the same lattice site as their progenitor and throughout their lifetime. Therefore, the β's produced by each decay pair should originate from the same pixel on the x-y plane of the CCD. The same procedure described below was performed to measure β decays from the sequence $^{210}\mathrm{Pb} \longrightarrow {}^{210}\mathrm{Bi} + \beta^{-} \longrightarrow {}^{210}\mathrm{Po} + \beta^{-}$.

The procedure starts by searching for the end-points of the β tracks. The pixel in the cluster with the maximum signal is used as a seed point and for every pixel of the cluster we compute the length of the shortest path to the seed point. The pixel with the greatest distance is taken as the first end-point of the track. Finally, we recompute the distance of every pixel from the first end-point, and take the pixel with the largest distance as the second end-point of the cluster. To find a β decay sequence, we calculate the distance from the end-points of every β cluster in an image to the end-points of every β cluster in later images. For every pair of clusters we have four distances corresponding to each end-point combination. The minimum of these distances is defined as the cluster distance. The pair is considered a candidate for a decay sequence if the distance of clusters is smaller than 20 pixels and the clusters have at least one pixel in common. To reduce the number of accidental pairs, we impose additional criteria on the energy of the clusters and their time separation. For the $^{32}\mathrm{Si} - {}^{32}\mathrm{P}$ sequence search, we require that the energy of the first (second) cluster to be $< 230\,\mathrm{keV}$ ($< 1.8\,\mathrm{MeV}$). We also require the time separation between the clusters of each pair to be less than 70 days (five half-lives of the daughter nuclei). Monte Carlo simulations were performed to estimate the pair selection efficiency (see [6]). Using these criteria, we found 16 candidates pairs in the data. No candidate was found in the $^{210}\mathrm{Pb} - {}^{210}\mathrm{Bi}$ search.

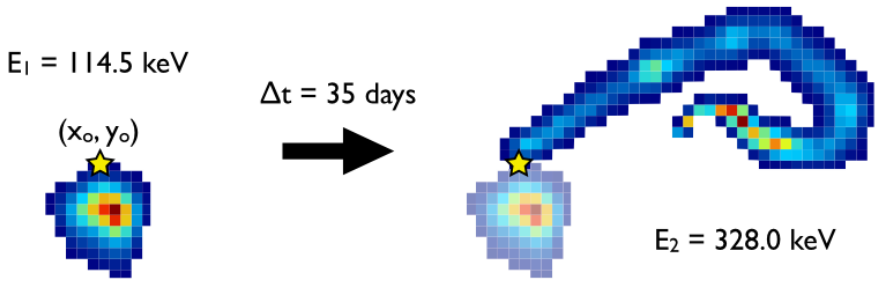

Figure 4. Candidate β decay sequence in data.

Analysis method	Isotope(s)	Tracer for	Bulk rate $kg^{-1}d^{-1}$	Surface rate $cm^{-2}d^{-1}$
α spectroscopy	^{210}Po	^{210}Pb	< 37	$0.011 \pm 0.004, 0.078 \pm 0.010$
	^{234}U + ^{230}Th + ^{226}Ra	^{238}U	< 5 (4 ppt)	-
	^{224}Ra – ^{220}Ra – ^{216}Po	^{232}Th	< 15 (43 ppt)	-
β spatial coincidence	^{32}Si – ^{32}P	^{32}Si	80^{+110}_{-65}	-
	^{210}Pb – ^{210}Bi	^{210}Pb	< 33	-

Table 1. All values are 95%CL upper limits or intervals, except for the ^{210}Po surface rate, where uncertainties are 1-σ. The two measurements of the ^{210}Po surface rate correspond to the two (back, front) CCD surfaces.

5. Conclusion

In this analysis we presented methods to measure the radioactive contamination in the CCDs of the DAMIC experiment. Thanks to the high spatial resolution of the detector, it is possible to distinguish α particles from the CCD's bulk or surface, which helps to indicate the origin of the background. A search for time-space correlations between β particles observed in different images was also realized. That latter analysis, concerning in particular the case of the ^{32}Si decay, is crucial for the current and future dark matter silicon-based detectors. In fact, the presence of the low energy β decay of this cosmogenic isotope may impose additional constrains on the next generation WIMP searches with high-purity silicon detectors, including the identification of a source of silicon with low ^{32}Si content to fabricate the detector and the requirement of $^{32}\mathrm{Si}-{}^{32}\mathrm{P}$ single-event identification for background suppression. Table 1 summarizes quantitatively all searches carried out in this analysis.

Finally, the current levels of radioactive contamination will allow DAMIC100, a 100 g detector currently under development, to probe WIMP-nucleon spin-independent interaction cross-section as small as 10^{-5}pb for WIMPs with masses as low as $2\,\mathrm{GeV.c}^{-2}$.

References

[1] JBarreto J *et al* 2012 *Phys. Lett.* **B711** 264
[2] Jungman G *et al* 1996 *Phys. Rept.* **267** 195
[3] Zurek K 2014 *Phys. Rept* **537** 91
[4] Groom D *et al* 2003 *IEEE Trans. Electron Dev.* **50** 225
[5] Chavarria A *et al* 2015 *Phys. Procedia* **61** 21
[6] Aguilar-Arevalo A *et al* 2015 *JINST* **10** P08014
[7] Estrada J *et al* 2011 *Nucl. Instrum. Meth. Phys. Res.* **A665** 90
[8] Agnese R *et al* 2013 *Phys. Rev. Lett.* **111** 251301